Deciphering the mitochondrial genome of *Oikopleura dioica* (Chordata: Tunicata: Appendicularia)

Yael Klirs[1], Maria Novosolov[1,2], Carmela Gissi[3,4,5], Rade Garić[6], Tal Pupko[7], Thomas Stach[8], Dorothée Huchon[1,9]

[1]School of Zoology, George S. Wise Faculty of Life Sciences, Tel Aviv University, Tel Aviv 6997801, Israel

[2]GeoGenetics Centre, GLOBE Institute, Faculty of Health and Medical Sciences, University of Copenhagen, Copenhagen, Denmark.

[3]Department of Biosciences, Biotechnology and Environment, University of Bari Aldo Moro, 70126 Bari, Italy

[4]Institute of Biomembranes, Bioenergetics and Molecular Biotechnologies, Consiglio Nazionale delle Ricerche, 70126 Bari, Italy

[5]CoNISMa, Consorzio Nazionale Interuniversitario per le Scienze del Mare, 00196 Roma, Italy

[6]Institute for Marine and Coastal Research, University of Dubrovnik, Kneza D. Jude 12, 20000 Dubrovnik, Croatia

[7]The Shmunis School of Biomedicine and Cancer Research, George S. Wise Faculty of Life Sciences, Tel Aviv University, Tel Aviv, 6997801 Israel

[8]Department of Molecular Parasitology, Institute of Biology, Humboldt-Universität zu Berlin, Berlin, Germany

[9]The Steinhardt Museum of Natural History and National Research Center, Tel Aviv University, Tel Aviv 6997801, Israel

ORCID IDs: 0009-0006-2572-0612 (Yael Klirs) 0000-0002-4034-3441 (Maria Novosolov), 0000-0002-2269-079X (Carmela Gissi), 0000-0001-6477-5559 (Rade Garić), 0000-0001-9463-2575 (Tal Pupko), 0000-0001-5461-9069 (Thomas Stach), 0000-0002-5047-244X (Dorothée Huchon).

* Author for Correspondence: Dorothée Huchon, School of Zoology, George S. Wise Faculty of Life Sciences, Tel Aviv University, Tel Aviv 6997801, Israel, +972 36409817, huchond@tauex.tau.ac.il

Abstract

Sequencing the mitochondrial genome of the tunicate *Oikopleura dioica* is a challenging task because of the presence of long poly-T/A homopolymer stretches, which impair sequencing and assembly. Here, we report the sequencing and annotation of the majority of the mitochondrial genome of *O. dioica* by combining several DNA and amplicon reads obtained by Illumina and MinIon Oxford Nanopore Technologies (ONT) with public RNA sequences. We document extensive RNA editing, since all homopolymer stretches present in the mitochondrial DNA correspond to 6U-regions in the mitochondrial RNA. Out of the 13 canonical protein-coding genes, we were able to detect eight plus an unassigned ORF, which lacked sequence similarity to canonical mitochondrial protein-coding genes. We showed that the *nad3* gene has been transferred to the nucleus and acquired a mitochondria-targeting signal. In addition to two very short rRNAs, we could only identify a single tRNA (tRNA-Met), suggesting multiple losses of tRNA genes, supported by a corresponding loss of mitochondrial aminoacyl-tRNA synthetases in the nuclear genome.

Based on the eight canonical protein-coding genes identified, we reconstructed maximum likelihood and Bayesian phylogenetic trees and inferred an extreme evolutionary rate of this mitochondrial genome. However, the phylogenetic position of appendicularians among tunicates could not be accurately determined.

Keywords

mtDNA, phylogenomics, Oxford Nanopore Technologies, RNA editing, tRNA loss, Mitochondrial-nuclear gene transfer

Significance

Sequencing and annotating the mitochondrial genome of fast-evolving organisms is difficult because they often present unusual characteristics. The tunicate *O. dioica* is a model species for understanding tunicate and chordate genome evolution. However, no complete annotated mitochondrial genome for this species has been published to date. Here, we determined the major part of the mitochondrial genome of *O. dioica*. Our results indicate the presence of highly modified rRNA genes and the absence of all tRNAs except tRNA-Met. Moreover, we show that the mitochondrial genome undergoes editing at the RNA level. Our study demonstrates that a combination of public RNA data and DNA from long-and short-read sequencing platforms significantly improves our ability to study mitochondrial genomes with atypical characteristics.

Introduction

Most mitochondrial genomes of Bilateria are circular DNA molecules of approximately 14-19 kb in length, characterized by the absence of introns and the presence of only short intergenic regions (Lavrov and Pett 2016). These genomes typically contain 37 genes: 13 protein-coding genes: ATP synthase subunits 6 and 8 (*atp6* and *atp8*), cytochrome oxidase subunits (*cox1, cox2, cox3*), cytochrome b (*cytb*), and dehydrogenase subunits (*nad1, nad2, nad3, nad4, nad5, nad6*, and *nad4L*); two ribosomal genes (rRNA): small-subunit (*rns*) and large-subunit (*rnl*) and ~22 tRNAs (Boore 1999; Gissi, et al. 2008; Rubinstein, et al. 2013). However, bilaterian mitochondrial genomes are substantially diverse in their structure, organization, evolutionary rate, and genetic code (Lavrov 2007).

Tunicate mitochondrial genomes are fast evolving, both in terms of substitutions (Singh, et al. 2009) and genome rearrangements (Gissi, et al. 2008; Stach, et al. 2010). As a result of this high rearrangement rate, there is no standard tunicate mitochondrial gene order. In addition, the ascidian mitochondrial genetic code differs from the vertebrate one. Of note, the "ascidian" genetic code, which was initially determined based on the mitochondrial sequences of *Halocynthia roretzi* and *Pyura stolonifera* (Durrheim, et al. 1993; Yokobori, et al. 1993), seems to be valid for all other tunicate classes (Pichon, et al. 2019).

Tunicata are divided into three classes: Ascidiacea, Thaliacea, and Appendicularia. Appendicularia is a key class for understanding tunicate and chordate genome evolution, as it is an early diverging clade within tunicates. *Oikopleura dioica* is a frequent model tunicate for the Appendicularia class in developmental biology, evolutionary biology, and comparative genomics research (Delsuc, et al. 2006; Nishida 2008). Despite the importance of this clade, no complete annotated appendicularian mitochondrial genome is currently available in public databases. One non-annotated mitochondrial genome of *O. dioica* from Okinawa Japan is available (accession OU015571; 9,225 bp; (Bliznina, et al. 2021)).

The mitochondrial genome of *O. dioica* from Norway has been partially reconstructed by Denoeud *et al.* (2010) from genomic DNA and EST data. However, the obtained mitochondrial contigs of this genome are not publicly available. This genome has been inferred to harbor long poly-T/A stretches interrupting the open reading frames (ORFs) and it has been proposed that these interrupted ORFs are corrected by RNA editing (Denoeud, et al. 2010). Such homopolymer stretches can neither be sequenced using Sanger sequencing nor using Illumina short-read sequencing, since they are error hot spots for the DNA polymerases used in these sequencing techniques. Thus, together with the difficulty in isolation and identification of appendicularian species, this peculiarity explains the paucity of publicly available mitochondrial data for *O. dioica*. Annotation of the resulting genome is also expected to be challenging, due to RNA editing. RNA editing describes modifications such as insertions, deletions, and base substitutions of RNA transcripts. As a result, the RNA and computationally inferred protein sequences differ from the DNA template (Gott and Emeson 2000). To complicate matters, in *O. dioica* RNA editing seems to be prevalent in the same regions that are hard to sequence, i.e., the poly-T/A stretches. These stretches appear as 6U-sites in mitochondrial RNA sequences, regardless of the number of T/A at the DNA level (Denoeud, et al. 2010).

The phylogenetic analyses performed by Denoeud *et al.* (2010) concluded that *O. dioica* mitochondrial protein-coding genes are very fast evolving, even when compared to the already high rate of other tunicate mitochondrial genomes. Using a combination of PCR and EST mapping approaches they determined the order of nine out of the 13 mitochondrial protein-coding genes: *cox3, nad1, cox1, cytb,* a putative *nad2, atp6, cox2, nad5,* along a large mitochondrial contig and *nad4* on a separate contig. They did not identify any tRNA or rRNA genes. Unfortunately, the mitochondrial contigs obtained by Denoeud *et al*. (2010) have not

been deposited in public databases and only the raw ESTs data are available in the Oikobase database (Danks, et al. 2012).

A draft mitochondrial genome scaffold of *O. dioica* from Okinawa (Japan) has been published by Bliznina, et al. (2021) (accession OU015571; 9,225 bp), with the annotation reported only in the publication (Figure 7 of their article). The annotation obtained is, however, preliminary as several genes contain stop codons and frameshifts. Unlike Denoeud, et al. (2010), the mitochondrial genome is presented as a circular molecule that encompasses seven mitochondrial genes (Bliznina, et al. 2021). The mitochondrial gene order resembles the order from Figure S4 of Denoeud, et al. (2010). Yet, some differences exist. First, the *nad2* and *nad5* genes are missing from the annotation of Bliznina, et al. (2021). Second, the *rnl* and four tRNAs: tRNA-Met, tRNA-Trp, tRNA-Ala, and tRNA-His are annotated. Third, they identified a LAGLIDADG homing endonuclease in the middle of the *cox1* gene (Figure 7 of Bliznina et al. 2021). It should be noted that *O. dioica* from Okinawa most likely represents a different species from *O. dioica* from Norway (Masunaga, et al. 2022).

Here, we determine the major part of the mitochondrial genome sequence of *O. dioica* from Norway, its gene content and its order. We observe substantial gene loss compared to other metazoan mitochondrial genomes and provide evidence for extensive RNA editing.

Results

Sequencing the Mitochondrial Genome

DNA extracted from *O. dioica* individuals from Norway was sent to Illumina sequencing. Since, it was impossible to assemble these reads because of the prevalence of homopolymers (poly-T or poly-A stretches), we next performed long-read sequencing using Oxford Nanopore Technology (ONT) sequencing. However, in this case, the flow-cell pores became blocked within an hour (Minion sequencing was performed twice by different companies), resulting in too little data for reliable assembly. Therefore, we PCR-amplified the mitochondrial genome in 12 fragments (supplementary Fig. S1, Supplementary Material online) and sequenced all barcoded fragments using a single ONT flow cell. Primers were designed based on the *O. dioica* EST and RNA data available in public databases (see Methods and supplementary table S1, Supplementary Material online). We successfully assembled each PCR fragment (except one), and using the Illumina data, we obtained a single contig. Unfortunately, we could not circularize the genome because we could not entirely assemble one fragment. The length of *O. dioica* mitochondrial contig assembled is 18,390 bp (Figure 1). This genome size is larger than the average of other tunicates, 14,808 ± 821 bp, and compatible with the PCR prediction of a ~19,000 bp genome (supplementary table S1, Supplementary Material online).

Multiple instances of poly-T/A stretches were found in the assembled contig (Figure 1, supplementary Fig. S2, Supplementary Material online). The exact number of either A/T repeats within poly-T/A regions could not be accurately determined. These stretches are too long to be fully contained in the short Illumina sequences (Ari and Arikan 2016), while ONT basecallers do not accurately determine the length of homopolymers (Wick, et al. 2019). Moreover, the length of homopolymers is correctly resolved up to a length of 11 bp in R10.4 flow cell (Sereika, et al. 2022), while in the R9.4.1 flow cell, a good accuracy (70% errorless)

is observed only in homopolymers up to 5 bp (Delahaye and Nicolas 2021). However, in our case, the length of the 65 poly-T/A stretches found in the mitochondrial sequence ranged from 2 to 509 bp, with an average of 143 ± 103.5 bp (See Methods, supplementary table S2, Supplementary Material online), which is considerably larger. Moreover, it has been observed that regions harboring inverted repeats are poorly sequenced using ONT (Spealman, et al. 2020). When in a PCR-fragment a poly-A region is followed by a poly-T region, these two homopolymers can form structures similar to inverted repeats, thus disrupting ONT sequencing. In addition, Taq polymerase slippage errors can further contribute to uncertainty associated with the length of long homopolymers. All these factors contribute to heterogeneity among ONT reads that map to the same mitochondrial locus harboring a poly-T/A region. One such example is shown in Figure 2. Note, that these stretches are sometimes imperfect, i.e., there may be a few G residues within a poly-A stretch or a few C residues with a poly-T stretch (Figure 2). These G and C residues are unlikely to reflect ONT sequencing errors, as they could sometimes be verified using Illumina reads. In total, these poly-T/A stretches span ~9,200 bp. This suggests that while the total mitochondrial genome size is longer than in other tunicates, the mitochondrial genome without the poly-T/A stretches is, in fact, shorter.

Evidence for rRNA Editing

A total of 65 poly-T/A sites were found in the assembled *O. dioica* mitochondrial genome. By mapping (1) the mitochondrial transcripts identified from the EST from Norway, and (2) the RNA contigs assembled from publicly available RNA reads from mainland Japan (Wang, et al. 2015) and the North Sea (Raghavan, et al. 2023) onto the DNA sequence assembled from the ONT reads, we were able to confirm the editing of 59 of these 65 poly-T/A sites to 6U-sites (see an example in Figure 2 and supplementary table S2, Supplementary Material

online). For the remaining 6 sites, no direct RNA evidence for editing exists as we could not detect RNA reads or ESTs that mapped to the corresponding region. These poly-T/A stretches are present both in coding and noncoding mitochondrial DNA regions. Specifically, we observed that exactly six consecutive U residues (6U-sites) in the RNA corresponded to a poly-T stretch in the DNA sequence. These results suggest that the longer U stretches in the pre-mRNA are edited, resulting in only shorter stretches of 6U. The exact nature of this RNA editing is unknown. It is, however, remarkable that protein-coding genes as well as the two rRNAs and the tRNA-Met only include poly-T regions and not poly-A regions. When poly-A regions are found on the direct strand, it indicates that the genes are encoded on the reverse strand. We detected a few instances of EST reads that include a poly-U stretch, i.e., before the excision of poly-U to 6U. These observations suggest that the shortening of the poly-U stretch, which is necessary to recover the reading frame, occurs at the RNA level co-transcriptionally or very fast after the synthesis of the precursor transcript.

Interestingly we noticed that while poly-T regions are present within all genes, the genes often end with a poly-A. The poly-A ending is part of the TAA stop codon in most protein-coding genes, except for *cox1*, which has a TAG stop codon (Table 1). The contigs assembled from RNA reads support the view that these poly-A stretches are reduced to 6A in the mRNA. Similarly, we noticed that a poly-A stretch is often present in the DNA before the start of a protein-coding gene (Figure 1). No conserved sequence motif could be identified around the poly-T/A stretches. The only major departure we could detect around the poly-T/A stretches is the absence of cytosine just after the 6T site. No other signal could be identified (Supplementary Fig. S3, Supplementary Material online).

Oikopleura dioica Mitochondrial Genome Sequence and Structure

Figure 1 presents the assembled mitochondrial genome of *O. dioica*. We could not determine the sequence in the region labeled as "Gap" between the *nad5* and *rnl* genes, probably because of the presence of secondary structures that impaired sequencing. Running the PCR product of fragment 12 on a gel suggests that the length of the "Gap" region is approximately 400 bp (supplementary Fig S1, Supplementary Material online). However, the fact that we could amplify this missing region using primers from both sides of the gap suggests that the genome is circular. Notably, although we could not assemble the entire fragment 12, the ONT-contigs we obtained allowed us to determine the end of the *nad5* gene and the *nad4-rnl* region, supporting the view that we amplified the correct region of the mitochondrial genome. The circularity of the mitochondrial genome is in line with Bliznina, et al. (2021).

Gene Content and Gene Loss in *O. dioica* Mitochondrial Genome

Most tunicate mitochondrial genomes encompass 13 protein-coding genes, two rRNA genes, and 24 tRNA genes that are encoded on the same strand (Shenkar, et al. 2016; Singh, et al. 2009). Surprisingly, in the mitochondrial genome of *O. dioica* we could only identify eight canonical protein-coding genes: ATP synthase subunit 6, subunits 1-3 of cytochrome c oxidase (*cox*), cytochrome *b* (*cytb*), and NAD dehydrogenase (*nad*) 1, 4, and 5. In addition to the two rRNA genes encoding the small and large subunits, we could identify a single tRNA gene, tRNA-Met (Figure 1, Table 1). The genes *cox1, cox2, cox3, cytb, nad1, nad5*, and tRNA-Met (UAU) are encoded on the forward strand, while *atp6, nad4, rns, rnl,* and an unidentified protein-coding gene named *ODI_mt_ORF196* (see below) are encoded on the reverse strand (Table

Table 1). No incomplete stop codons were found (Table 1). Moreover, no LAGLIDADG ORF was found to be encoded within the *cox1* gene. These results suggest the loss of five protein-coding genes: *atp8, nad 2, 3, 4L,* and *6* and all tRNA genes except for tRNA-Met.

An additional mitochondrial protein-coding gene was identified following a Blastn search of the obtained mitochondrial sequence against the EST data available in Oikobase (Danks, et al. 2012). Notably, programs such as “Find ORFs” (implanted in Geneious Prime v.2023.2.1.) are inapplicable for this mitochondrial genome, because of the extreme fast rate of evolution and the numerous poly-T/A stretches that disrupt the reading frames of protein-coding genes. This additional ORF is 1,426 bp long and does not show any significant sequence similarity to any known protein-coding gene present in NCBI public database (i.e., based on Blastp searches). We thus dubbed it gene “*ODI_mt_ORF196*” based on its amino-acid length (Figure 1, Table 1). This protein was inferred to have six transmembrane domains and, based on its position, it corresponds to the putative *nad2* gene identified by Denoeud, et al. (2010). An Alpha fold-based prediction of this gene (supplementary Fig. S4, Supplementary Material online) was used as query against multiple protein structure databases: AlphaFold/UniProt50 v4, AlphaFold/Swiss-Prot v4, AlphaFold/Proteome v4, CATH50 4.3.0, MGnify-ESM30 v1, PDB100 2201222, GMGCL 2204 from Foldseek (van Kempen, et al. 2024). No significant structural hits were obtained.

We identified the two rRNA genes, *rns* and *rnl*, by searching for highly transcribed regions along unannotated regions of the assembled genome. Two noncoding regions were found to be highly expressed based on Illumina RNA read mapping (supplementary Fig. S5, Supplementary Material online). Further support for the transcription of these regions is their presence in the EST data. Specifically, the longer expressed non-coding region that resides between the “gap region” and the *nad4* gene was assumed to be the *rnl* gene. This annotation is supported by RNA structure similarity between the putative *rnl* and structure model profile of *rnl* genes, as implemented in Mitos2 (Donath, et al. 2019). The second, shorter expressed noncoding region, located between the *atp6* and the *cox2* genes, was annotated as *rns*, although no structural similarity was found between this sequence and *rns* structure profile in

Mitos2. Both the *rnl* and *rns* genes were found to be extremely short: 291 and 232 bp, respectively, compared to 1,129 and 660 bp in the model tunicate *Ciona intestinalis* (see also Table 1).

We could identify a single tRNA gene, tRNA-Met (UAU). This tRNA presents a typical secondary cloverleaf structure (supplementary Fig. S6, Supplementary Material online), and UAU anti-codon, corresponding to a methionine codon according to the ascidian mitochondrial code. Unlike in Bliznina, et al. (2021) no other tRNAs were identified.

Aminoacyl-tRNA Synthetase (aaRS) Profiling

We used hidden Markov models (HMMs) to identify nuclear-encoded aaRSs in published sequences of *O. dioica* and few other chordate representatives (Figure 3, supplementary table S4, Supplementary Material online). We found the presence of all cytosolic aaRSs in published proteomes of *O. dioica* (accessions: GCA_000209535, Norway and GCA_907165135, Okinawa) (Figure 3). However, in contrast to the other chordates investigated, *O. dioica* is inferred to have lost most of the mitochondrial aaRSs except for aaRS-Gly (G), aaRS-Phe (F), and aaRS-Met (M). Likewise, the mitochondrial aaRS-Val (V) is absent in the tunicates *C. intestinalis* (GCA_000224145) and *Styela clava* (GCF_000001405), and the mitochondrial aaRS-Lys (K) and aaRS-Thr (T) are absent in all species included in this comparison. Furthermore, *O. dioica* encodes two copies of aaRS-Gly (one cytosolic and the other mitochondrial) while the other chordates encode only a single copy that functions both in the cytosol and the mitochondrion, suggesting a duplication event in the lineage leading to appendicularians.

Gene Transfer to the Mitochondrial Genome

HMMs were used to search for the missing canonical mitochondrially-encoded genes (i.e., *nad2*, nad3, *nad4L*, *nad6*, and *atp8*) in the nuclear genome. Using these models, we found a protein sequence with a significant similarity (E-value < 5e-07) to the NAD3 model in the two published proteomes of *O. dioica* (proteins CAG5094752 and CBY12996 for the Norwegian and Okinawan genomes, respectively). A domain search confirmed that the protein sequence identified includes a NAD-ubiquinone/plastoquinone oxidoreductase, chain 3 domain (Cdsearch (Wang, et al. 2022) search using the CAG5094752 and CBY12996 protein sequences as queries against the CDD v3.21 database yielded E-values of 4.94e-03 and 3.80e-03, respectively). This protein was predicted to include two putative transmembrane domains, in support of its role in the electron transport chain (supplementary Fig. S7, Supplementary Material online). This protein-coding gene was found to be encoded on the X specific region of the X chromosome of *O. dioica* and to harbor three introns. Conversely, no nuclear-encoded protein showing significant similarity to the NAD3 model was found in the proteomes of *C. intestinalis*, *S. clava* and *H. sapiens*.

To confirm that the identified NAD3 proteins of the Norwegian and Japanese *O. dioica* are expressed in the mitochondria we search for the presence of mitochondrial target peptides. A significant target peptide signal was found in these putative NAD3 proteins with a likelihood above 0.89. We could not confirm the transfer of other missing genes (i.e., *nad2*, *nad4L*, *nad6*, and *atp8*) to the nuclear genome: this can be due to the fast-evolutionary rate of *O. dioica* and the short length of these proteins (150-152 amino-acid), or to the incompleteness of proteomic data for *O. dioica*.

Phylogenetic Reconstructions

Phylogenetic reconstructions were performed using two datasets. In the first, *Doliolum nationalis* was the sole representative of the tunicate class Thaliacea. The second dataset differed from the first by including two additional thaliacean sequences: the fast-evolving sequences of *Salpa thompsoni* and *Salpa fusiformis* (supplementary table S4, Supplementary Material online). Phylogenetic trees were reconstructed under the maximum likelihood (ML) criterion using various models of sequence evolution implemented in IQtree (Minh, et al. 2020; Wang, et al. 2017), including complex models (i.e., MtZoa+F+G+I, MtZoa+EHO+F+G+I, Poisson+C10+G, Poisson+C20+G) and under the Bayesian CAT model implemented in Phylobayes (Lartillot and Philippe 2004). In all trees the monophyly of tunicates was supported with maximal support (bootstrap percentage (BP) = 100, posterior probability (PP) = 1.0), however, the position of *O. dioica* was highly variable depending on the dataset and the evolutionary model chosen (Figure 4, supplementary Fig. S8 A-J, Supplementary Material online). When the tree was reconstructed without members of the *Salpa* genus, *O. dioica* was the first tunicate to diverge when using the MtZoa+F+G+I or the MtZoa+EHO+F+G+I models (see Figure 4 and supplementary Fig. S8 A, Supplementary Material online). Remarkably, the branch support values for the early divergence of *O. dioica* were low (BP < 50%). Conversely, support for the monophyly of accepted tunicate clades (i.e., Stolidobranchia and Thaliacea+Phlebobranchia+Aplousobranchia) was moderate to high (BP = 60-93%). When using more complex models such as the Poisson+C20+G (supplementary Fig. S8 C, Supplementary Material online) or the Bayesian CAT model (supplementary Fig. S8 H-J, Supplementary Material online), *O. dioica* branched within Stolidobranchia. This positioning and the resulting relationships among Stolidibranchia clades were not supported (BP < 50%; PP < 0.5). When members of the genus *Salpa* were included in the phylogenetic analyses, *O. dioica* systematically grouped with the *Salpa* members

except when using the most complex Poisson+C20+G ML model (supplementary Fig. S8 G, Supplementary Material online). Interestingly, support for this relationship decreased with the complexity of the ML model used (BP = 85%, MtZOA+G+F; BP = 77%, MtZoa+EHO+G+F, BP = 51%, Poisson+C10+G) (supplementary Fig. S7 D-F, Supplementary Material online). In the tree reconstructed with the Poisson+20+G model, the Thaliacea monophyly was recovered (BP = 59%) but *O. dioica* branched within Stolidobranchia, and basal relationships within tunicates were not supported (BP < 50%). When using the Bayesian CAT model, the phylogenetic position of *O. dioica* could not be resolved when *Salpa* was included. Specifically, convergence parameters suggested that convergence was achieved, however, different topologies were obtained depending on the chains considered. With chains 1, 2 and 3 the Thaliacea monophyly was recovered but not supported (PP = 0.53). When chains 1, 2, and 4 were considered, *Salpa* and *O. dioica* were found to be sister clade (PP = 0.57) (supplementary Fig. S8 I-J, Supplementary Material online).

Discussion

The mitochondrial genome of *O. dioica* appears extremely divergent and fast-evolving. It is characterized by the presence of numerous poly-T/A stretches undergoing RNA editing. A few canonical metazoan mitochondrial protein genes and almost all tRNA genes are absent from the genome, there is a substantial reduction in the size of the rRNA genes, and there is evidence of a protein-coding gene transfer to the nuclear genome. Such high mitochondrial genome plasticity characterizes fast-evolving animal clades (Pett, et al. 2011; Yahalomi, et al. 2017).

Protein-Coding Genes

Five canonical protein-coding genes are absent (*atp8, nad2, nad3, nad4L,* and *nad6*) in the mitochondrial genome of *O. dioica*, four of which were not identified in the nuclear genome (i.e., all excluding *nad3*). These four genes may be encoded in either the mitochondrial or the nuclear genome, but we were unable to identify them. Indeed, the *O. dioica* mitochondrial and nuclear genomes are extremely fast evolving, and consequently, these genes may have been missed by algorithms for remote homology detection, including HMM searches. Notably, these missing genes (*atp8, nad2, nad4L,* and *nad6*) are among the fastest evolving mitochondrial genes (Castellana, et al. 2011; Pesole, et al. 1999). The unassigned gene *ODI_mt_ORF196* is predicted to encode a protein harboring four alpha helices (supplementary figure S4, supplementary material online), unlike all other missing proteins in tunicates: the NDH2 protein of most metazoans harbors six alpha helices and the other canonical mitochondrial proteins are predicted to harbor three or fewer alpha helices (The UniProt The UniProt Consortium 2022). Moreover, none of the methods used (Blastp, HMMer, and Cdsearch) detected a significant similarity with any other canonical proteins. We thus refrained from annotating this gene as one of the four missing gene, although Denoeud *et al*. (2010) annotated this gene as *nad2*.

After removing poly-T/A regions, the largest non-coding region identified is 206 bp (between *ODI_mt_ORF196* and *cytb*) and it is possible that at least one among the *atp8* and *nad4L* genes, which are shorter than 300 bp in most tunicates, are encoded within this region. The *atp8* gene, in particular, has been overlooked in the past from the original annotation of several mitochondrial genomes (e.g. Helfenbein, et al. 2004; Hoffmann, et al. 1992; Le, et al. 2002; Okimoto, et al. 1992), including tunicates (Yokobori, et al. 1999; Yokobori, et al. 2003) and was then identified in ascidians following mitochondrial EST analyses (Gissi, et al. 2004; Gissi and Pesole 2003).

Our results suggest that *nad3* has been relocated to the nuclear genome. While this is the first evidence for relocation of this mitochondrial gene to the nucleus in animals, a case of nuclear *nad3* has been reported in the green alga *Chlamydomonas reinhardtii* together with the transfer of *nad4L* (Cardol, et al. 2006). Similar transfers to the nuclear genome have been described for other animal mitochondrial genes, for example, the *atp6* and *atp9* genes of the ctenophore *Mnemiopsis leidyi* (Pett, et al. 2011), and the mitochondrial gene *atp9* in the demosponge *Amphimedon queenslandica* (Erpenbeck, et al. 2006). Short ORFs are more difficult to identify than long ones, and because *atp8* and *nad4L* are relatively short, it is possibly that this factor, in additional to their high rate of evolution, impaired their identification. The fact that *nad6* was detected neither in the mitochondrial genome nor in the nuclear one, is more surprising. This gene is longer (450.9 bp ± 20.2 bp in other tunicates), and except for the gene ODI-mt-*ORF196*, no other putative ORFs longer than 300 bp were detected. The possible incompleteness of the two public *O. dioica* assemblies and the inferred proteomes, or the specific criteria and bioinformatic pipeline used to annotate the protein genes in these nuclear assemblies, could also explain the failure to identify *nad6*, *atp8* and *nad4L* in the available nuclear assemblies.

A third explanation could be that the genes that we could not identify have been fused with other mitochondrial genes. For example, the ORF we annotated as *atp6* could include regions corresponding to both *atp6* and *atp8*. An example of ORF fusion is found in the *cox*1/2 gene of amoebas (e.g., Lonergan and Gray 1996). However, this explanation is unlikely in our case since all *O. dioica* ORFs are shorter than their tunicate counterparts (Table 1), while in the case of a fusion, we would expect these ORFs to be longer.

rRNA Genes

Tunicate rRNA genes are known to be poorly conserved. As a case in point, the boundaries of tunicate mitochondrial rRNA genes are mostly inferred from the end and start of the flanking genes, indicating that the length estimates of rRNA genes are error-prone (Rubinstein, et al. 2013; Singh, et al. 2009). Only for the ascidians *Halocynthia roretzi* and *C. intestinalis*, some rRNA boundaries were tentatively better defined based on EST transcript data (Gissi and Pesole 2003). Although the two rRNA genes are retained in all tunicate mitochondrial genomes, they exhibit a great range of sizes. Tunicates present the shortest mitochondrial rRNA genes among chordates with lengths varying from 596 to 984 bp for *rns* and from 921 to 1,299 bp for *rnl* (Table 1). Both rRNAs are considerably shorter in *O. dioica,* with the *rns* and *rnl* being 242 bp and 215 bp, respectively, after the removal of the poly-T stretches (Table 1). Additionally, they have lost most structural similarity with other metazoan rRNA genes (HMM searches could only identify a part of the *rnl* gene). Interestingly, extreme mitochondrial rRNA reduction and lack of structural similarity are characteristics shared between appendicularians and ctenophores (Arafat, et al. 2018), another lineage with an extreme rate of mitochondrial genome evolution. We annotated the two rRNA regions as different genes because most mitochondrial genomes contain these two genes. However, given the absence of sequence similarity we cannot exclude the possibility that the *rns* region may be, instead, a fragment of the *rnl*. Indeed, in calcareous sponges and Placozoa, rRNA genes are fragmented and encoded on different regions of the mitochondrial genome (reviewed in Lavrov and Pett 2016). Of note, *trans*-splicing is unknown in animals.

tRNA Genes

Though most tunicates encode 24 tRNAs, their tRNA gene content is variable and ranges from 22-27 tRNAs (Iannelli, et al. 2007; Rubinstein, et al. 2013). Specifically, the loss and

acquisition of additional tRNA genes seem to be tolerated and the number of tRNA genes has been found to vary in a species-specific manner (Gissi, et al. 2008; Rubinstein, et al. 2013). In *O. dioica* the situation is again extreme as all tRNAs are absent except for the tRNA-Met (UAU).

Nuclear-encoded cytoplasmic tRNAs import to the mitochondria has evolved many times over the course of mitochondrial evolution (Adams and Palmer 2003). We thus assume that the missing mitochondrial tRNAs in *O. dioica* mitochondrial genome are now encoded in the nuclear genome and are imported to the mitochondria.

The retention of a single tRNA-Met in the mitochondrial genome, despite the loss of all other, or most, tRNAs, is not novel to appendicularians and has been observed in cnidarians, certain chaetognaths, and Keratosa sponges (Lavrov, et al. 2023). The conventional explanation is based on the fact that mitochondrial protein synthesis starts with N-formylmethionine, as in prokaryotes, instead of methionine, the initiating amino acid in eukaryotic cytosolic protein synthesis. The addition of a formyl group to methionine is catalyzed by the enzyme methionyl-tRNA formyltransferase (Bianchetti, et al. 1977). As found in prokaryotes, and in accordance with the prokaryotic endosymbiotic origin of mitochondria, this modification occurs not on free methionine but after methionine is loaded onto a specific tRNA, namely the initiator tRNA-fmet. Hence, it is usually assumed that the retained tRNA-Met in mitochondria is the initiator tRNA-fmet (e.g., Beagley, et al. 1998).

Interestingly, animal mitochondrial genomes usually keep tRNAs that are specific to their mitochondrial genetic codes. For example, most cnidarians retain the tRNA-Trp gene necessary for the translation of the UGA codon, which is a stop codon in the nuclear genetic code (Beagley, et al. 1998). In the mitochondrial genetic code of ascidians, four codons have a different assignment compared with the nuclear genetic code: methionine (AUA), tryptophan (UGA), and glycine (AGA and AGG). We thus expected the presence of a tRNA-

Trp (for the translation of the UGA codon) and a tRNA-Gly (to translate the codons AGA and AGG) in the mitochondrial genome of *O. dioica*. Therefore, we computed the codon frequency across all protein-coding genes of *O. dioica*, thus verifying the usage of all these AUA, UGA, AGA and AGG codons in the mitochondrial genome (supplementary table S5, Supplementary Material online). Indeed, it has been found that translation of the AGA and AGG codons to Gly improves the similarity between *O. dioica* and tunicate mitochondrial proteins, supporting the use of the ascidian mitochondrial genetic code in appendicularians (Pichon, et al. 2020). The presence of a cytosolic and a mitochondrial aaRS-Gly, observed while searching for mitochondrial aaRS in *O. dioica* nuclear genome, further supports the view that a specific mitochondrial tRNA recognizes the glycine AGA and AGG codons. As for the case of protein-coding genes, two explanations are possible for the lack of mitochondrial Gly and Trp tRNAs: either we failed to identify these tRNA genes in the sequenced mitochondrial genome, because of their very unusual secondary structure or because they are interrupted by poly T/A stretches, or these tRNAs are nuclear-encoded and imported from the cytosol. In support of the import scenario, it was found that among animals, both ctenophores and Myxozoa have lost all their mitochondrial tRNA but still use the UGA codon as tryptophan (Arafat, et al. 2018; Pett, et al. 2011; Yahalomi, et al. 2017).

Genome Editing of Poly-T/A Stretches

The sequencing of PCR fragments using ONT long-read allowed us to assemble a large part of the mitochondrial genome of *O. dioica*. It confirms the presence of numerous poly-T/A stretches in the DNA sequence that are reduced to 6U-sites in the RNA transcript. Because accurate sequencing of long homopolymers is currently infeasible with Sanger, Illumina (Ari and Arikan 2016) or Nanopore sequencing (Delahaye and Nicolas 2021; Sereika, et al. 2022), the length of T/A stretches in our assembly is unreliable. The average size of these regions is

likely slightly higher than that reported in the assembly because sequencing methods tend to underestimate the length of homopolymer stretches. Another source of uncertainty regarding the length of the homopolymer stretches stems from the fact that we sequenced amplicons obtained from DNA extracted from a pool of polymorphic individuals. Intra-species variation in the length of these stretches likely exists, further contributing to inference uncertainty.

What is the molecular mechanism underlying the editing to 6U-sites, and more specifically, how are these sites recognized? We could not identify a conserved sequence motif surrounding these sites (Supplementary Fig. S3, Supplementary Material online). Our analysis reveals the following general motif for the poly- T/A stretch (see Methods): (1) the 5'-end of this strand starts with a perfect 6T homopolymer; (2) downstream of this region, there is a poly-pyrimidine track whose length varies from 2 to 509 bases; (3) it ends when a purine. Only the poly-pyrimidine track is excised. We speculate that the perfect 6T motif in the upstream region may be the beginning of the recognition editing signal and that a purine marks its end. In between these motifs, the polypyrimidine track is excised. Notably, the enzymes involved in this excision mechanism are still unknown.

Another kind of editing was observed within the cytochrome *b* gene: instead of a perfect 6T motif, it starts with "TTTTTCTT", then there is the excised region, "AACTT", which is irregular as it contains two purines (supplementary Fig. S9, Supplementary Material online).

Mitochondrial genome editing is rare in animals, and it is usually limited to the insertion of a few bases (Lavrov, et al. 2016). Here we instead have a deletion of a large polypyrimidine region. The removal of such a long stretch at the RNA level is a characteristic of introns (Chorev and Carmel 2012). Spliceosomal introns are characterized by short signal sequences such as GT/AG and AT/AC (Berná and Alvarez-Valin 2014; Rogozin, et al. 2012). It seems that the RNA editing observed here is very different from such a splicing mechanism

as we could not find such motifs. Similarly, the poly-T/A stretches have no sequence similarity with self-splicing introns that have well-defined secondary structures (Waring and Davies 1984).

Trypanosomatid protists present a cleavage-ligation pathway through which multiple uridines can be deleted or inserted by a U-specific exonuclease and a terminal uridil transferase, respectively (Cruz-Reyes and Sollner-Webb 1996). This particular editing mechanism involves guide RNAs, which determine the number and positions of the U nucleotides deleted or inserted within the mitochondrial genome of these protists, e.g., *Leishmania tarentolae* (Connell, et al. 1997). Future studies are necessary to determine if some components of the editing mechanisms in these protists and in *O. dioica* are evolutionary related.

Appendicularians have classically been divided into three families Fritillariidae, Kowaleskiidae, and Oikopleuridae (Garić 2024). However preliminary results from our group suggest that Kowaleskiidae are members of the Fritillariidae (Garić, et al. 2018). The presence of edited homopolymer stretches has been mentioned for the COI gene of *O. vanhoeffeni* (Latour 2021). Interestingly, we have observed that large poly-T inserts are also present in members of the Fritillariidae, suggesting that this mitochondrial editing mechanism was present in the ancestor of Appendicularia (Garić, et al. 2018). Conversely, while examining published data from Naville et al. (Naville, et al. 2019), we identified a clade within Oikopleuridae, which includes the species *Bathochordaeus stygius*, *Mesochordaeus erythrocephalus*, and *Oikopleura longicauda* that do not harbor large poly-T/A stretches (Garić, et al. 2018), suggesting that this RNA editing mechanism may have been lost in Oikopleuridae. Additional genomic and transcriptomic data from a larger taxon sampling of appendicularians are needed to better understand the distribution and evolutionary dynamics of this editing mechanism.

EST and transcriptomic RNAseq data are available for *O. dioica* from Norway and mainland Japan, respectively. For the Norway sample, genomic data were obtained in this work, indicating the presence of RNA editing. To evaluate if the Poly-T stretches are conserved among *O. dioica* lineages, we compared the location of 6U-regions in the DNA and transcriptomic data from Norway and mainland Japan, respectively (Supplementary Fig. S2, Supplementary Material online). Our results suggest that while many of the 6U-loci are conserved, differences exist. For example, in the *cox1* gene, a 6U-site in the Norwegian sequence and a UUCUUU site in the Japanese sequence can be reliably aligned. These differences suggest that the poly-T/A stretches loci may not be conserved in the mitochondrial genomes of different populations or species. Of note, it was recently suggested that *O. dioica* from Japan and Norway represent different species (Masunaga, et al. 2022). The birth and death dynamics of these poly-T/A stretches will be better clarified when genomic and transcriptomic data from a larger appendicularian taxonomic sampling becomes available.

The fact that we could assemble large contigs encompassing several genes from RNA sequences indicated that the pre-mRNA transcripts in *O. dioica* are polycistronic. In vertebrates, it has been shown that the cleavage of tRNAs which flank protein-coding genes (named tRNA punctuation) is the mechanism that releases monocistronic or bicistronic mature mRNAs of mitochondrial coding genes from the large RNA precursor (Ojala, et al. 1981). In ascidians, the transcription and RNA maturation process of the mitochondrial genome has been reconstructed through EST analyses, showing that the main features of mitochondrial transcription are conserved between vertebrates and ascidians (*i.e.*, presence of polycistronic and immature transcripts, creation of stop codons by polyadenylation, tRNA signal punctuation, and rRNA transcript termination signals) (Gissi and Pesole 2003). Since most tRNAs are lost in *O. dioica*, a mechanism different from the tRNA signal punctuation is likely employed to release mature mRNAs.

The Phylogenetic Position of *O. dioica*

Based on both molecular (Delsuc, et al. 2018) and morphological (Braun, et al. 2020) analyses *O. dioica* was placed as the first diverging branch of the tunicates tree, however it was recognized that this placement, in molecular studies, may be a long-branch-attraction (LBA) artifact (Delsuc, et al. 2018). In our analysis, we found that the phylogenetic position of *O. dioica* was highly variable. The grouping of *O. dioica* and members of the genus *Salpa* is most likely an LBA artifact (Philippe, et al. 2005), however, even when the two *Salpa* representatives were removed from the phylogenetic analyses, the phylogenetic position of *O. dioica* was never well supported and depended on the model used. This suggests the fast-evolutionary rate of this species impedes the use of molecular markers to resolve its phylogenetic position. Again, the lack of phylogenetic signal in the mitochondrial dataset, which precludes the reconstruction of phylogenetic relationships at the phylum level, is a feature of fast-evolving species (Arafat, et al. 2018; Pett, et al. 2011; Yahalomi, et al. 2017).

Conclusions

We demonstrated that a combination of DNA and RNA data from long- and short-read sequencing could significantly improve our understanding of the structure and gene content of *O. dioica* mitochondrial genome.

The mitochondrial genome of *O. dioica* shows unique gene content and an extreme rate of sequence evolution. A total of 28 genes are missing, including *atp8*, *nad2*, *nad3* *nad4L*, *nad6*, and all tRNA genes except for tRNA-Met (UAU). The mitochondrial gene *nad3* was transferred to the nucleus, and harbors a mitochondrial target peptide. Further work is, however, needed to decipher the complete sequence of the mitochondrial genome and in particular to unravel the accurate sequence and length of the poly-T regions. Unfortunately, currently, no sequencing techniques allow us to perfectly sequence these regions, as the sequencing methods Illumina, ONT, and Sanger approaches failed to correctly sequence long polynucleotide regions. However, information obtained from the sequencing of PCR fragments helped us assembled a draft mitochondrial genome.

Because of the fast-evolutionary rate, we were unable to accurately determine the phylogenetic position of *O. dioica*. Of note, comparative genomic studies of *O. dioica* and additional members of the appendicularians are expected to provide us with a better understanding of the evolution of RNA editing in this group.

Materials and Methods

DNA Extraction, Sequencing and Assembly

Living specimens of *O. dioica* animals were provided by Sars International Centre for Marine Molecular Biology (SICMMB) (Bergen, Norway) in March 2019 and cultured at Humboldt-University zu Berlin (HU) following the methods detailed in Bouquet, et al. (2009). Ethanol-preserved samples were shipped to Tel-Aviv University. Genomic DNA was extracted from ~100 whole individuals following the protocol of Fulton (2012). About 100 ng were sent to the Technion sequencing center (Haifa) for Illumina sequencing (November 2019), the libraries were prepared using the TruSeq DNA Nano library prep kit (Illumina) and were sequenced on an Illumina Hiseq 2500 platform. Similarly, about 1μg of total DNA was sent to Hy Laboratories Ltd (Hylabs, Rehovot) for ONT sequencing using a MinION Mk 1 R9.4 flow cell with a MinION Mk1B device and 1D sequencing kits (May 2019). However, the ONT sequencing only provided 962 reads (mean length 750 bp). ONT sequencing was thus again performed using a different DNA extract and a different sequencing service (the Technion sequencing center) (on July 2019 and December 2021). The flow cell and device setting and sequencing kits were the same as previously. The first sequencing (July 2019) provided ~2 million reads (mean length 2,330 bp) but we could not assemble the mitochondrial genome using these data. *A posteriori,* we found that only ~600 reads mapped to the mitochondrial genome (mean length 300 bp) and that these reads only mapped to a few regions of the mitochondrial genome (data not shown). For this second ONT sequencing fragments around 3,000 bp were selected. Because we realized that mitochondrial DNA may be fragmented, we performed the last ONT sequencing (from December 2021) without fragment size selection. This ONT sequencing also provided only 3,144 reads (mean length 1,070 bp).

The Illumina 100 bp paired-ended reads were cleaned from adaptors using Cutadapt v.2.8 (Martin 2011) and assembled using IDBA-UD v.1.1.3 (Zhu, et al. 2010) using default parameters. Efforts to assemble the mitochondrial genome from these reads were unsuccessful because contigs were broken in the long poly-T regions.

Because whole genome sequencing using Illumina or ONT did not allow us to assemble a complete mitochondrial sequence we decided to amplify the mitochondrial genome into several PCR fragments. To do so we needed to design primers in conserved regions that did not include homopolymers. We used published RNA reads and EST sequences to identify mitochondrial genes and design primers.

Identification of Canonical Mitochondrial Protein Transcripts in Published RNA and EST Sequences

Illumina RNA reads from *O. dioica* specimens from Japan and the North Sea were downloaded from the National Center for Biotechnology Information (NCBI) (accessions: SRR1693762, SRR1693765, SRR1693766, and SRR1693767) (Wang, et al. 2015), and the European Nucleotide Archive (ENA) (accessions: SRR20015061) (Raghavan, et al. 2023), respectively. The reads were then assembled with IDBA-UD v.1.1.3 (Zhu, et al. 2010) using default parameters. tBlastn searches were conducted against the transcriptome assembly obtained using the amino acid sequences of the protein-coding genes of the mitochondrial genome of *Ciona robusta* (AJ517314) as query. The reads from Japan could be assembled in four contigs and will be referred to as “Japan” (supplementary Fig. S10 A, Supplementary Material online). These contigs were annotated with the webserver MITOS V2 (Donath, et al. 2019) The genes from the North Sea could be assembled in five contigs and will be referred to as “North Sea” (supplementary Fig. S10 B, Supplementary Material online). All contigs were annotated with the webserver MITOS V2 (Donath, et al. 2019).

Mapping Illumina DNA reads and the few ONT reads to these contigs confirmed the presence of homopolymers and also indicated that the Japanese *O. dioica* presented many substitutions when compared to our sample which originated from Norway. EST sequences from *O. dioica* samples from Norway were available in the OikoBase database (Danks, et al. 2012). For each mitochondrial ORF identified in the Illumina North Sea dataset, we mapped ~500 EST sequences to the reference. We next filtered the flanking regions of the extracted EST sequences against the UniVec Vector using Geneious Prime v.2023.2.1. The consensus sequences were extracted for each gene, which helped us determine the exact gene boundaries. We verified that all coding transcripts we identified could be successfully translated to protein using the ascidian or the invertebrate mitochondrial codes. We found that the ascidian genetic code yields proteins that have higher sequence similarity to mitochondrial proteins in other animals than when using the invertebrate genetic code, in agreement with Pichon, et al. (2020).

PCR Amplification, Sequencing and Assembly

Primers of ~ 30 bp with a TM ~ 60 C° were designed based on ORF assembled from the EST, accounting for the gene order inferred from the contigs (supplementary table S1, Supplementary Material online). Long PCRs were performed, with several primer combinations (one from each pair of contigs and in various orientations), to determine gene arrangements along the mitochondrial genome. Because of the high AT content of the genome, we were unable to design primers that would result in overlapping PCR fragments. Instead, we used the same region for forward and reverse primers, leading to non-overlapping fragments. The sequence of the primer region was confirmed using Illumina data. PCRs were performed in a 25µl volume with 2u of TaKaRa Ex-Taq polymerase (Cat.# RR001), 1X of Ex-Taq buffer, 1M of Betain, 0.2mM of dNTPs TaKaRa mixture, 0.5µM of each primer and

1μl *O. dioica* DNA extraction. The PCR program used: (a) long denaturation step at 95°c for 5 min; (b) 35 cycles of a short denaturation step at 95°c for 45 sec followed by an annealing plus elongation step at 68°c for 10 min; (c) a long elongation step at 72°c for 10 min. Reamplifications was performed to improve the PCR yield of some fragments. Reamplifications were performed using 1 μl of PCR products in place of genomic DNA. 12 PCR reactions were successful and sent to ONT sequencing (supplementary Fig. S1, Supplementary Material online). Each PCR product was barcoded and the sequencing was performed in May 2023 by the Technion Sequencing Center on an Oxford Nanopore MinION device (MinKNOW software v.22.12.7), using one R9.4.1 flow cell (Oxford Nanopore, cat no. FLO-MIN106D). The ONT reads obtained were filtered from adaptors using Porechop v.0.2.4 (Wick, et al. 2017) using the parameters -middle_threshold 85. Next, we assembled the trimmed ONT reads with Flye v.2.9.1 (Kolmogorov, et al. 2020) as implemented in Geneious Prime v.2023.2.1 with two rounds of polishing. The same parameters could not be used for all PCR fragments as in some cases, the assembly program returned an error message or failed to terminate. In these cases, other parameters were tested, e.g., if the default parameter “genome size” of 1,000 bp resulted in a failed run, we tried running the program with increasing values of genome size from 2,000 to 5,000 bp. If this also failed, we added the option “metagenome” or the option “reduced contig = 30”. Even with these modifications, the assembly of PCR fragment 12 was unsuccessful.

Many of the assembled contigs were palindromic, with the middle of the contig corresponding to the PCR primer. In this case, the consensus sequence was split into two halves, reads were mapped to each half (using Geneious Prime v.2023.2.1 with default options) and the region with the highest number of mapped reads was kept as the consensus sequence.

The entire mitochondrial sequence was determined by connecting the obtained contigs in their overlapping primer regions, i.e., the same primer region was the forward primer of one PCR fragment and the reverse primer on another fragment. The exact sequences of the primer regions were verified by mapping the Illumina reads to the assembled genome sequence.

Annotation of the Mitochondrial Genome

Protein-coding genes

Gene annotation was based on Blast search against the NCBI databases and was confirmed using MITOS v.2 (Donath, et al. 2019). The end positions of protein-coding genes were verified using EST data (the presence of a poly-A region after the stop codon). The start codon was determined by searching for the first start codon upstream of the region that corresponded to the EST data.

rRNAs

The mapping of Illumina RNA reads from Japan (SRR1693762, SRR1693765, SRR1693766, SRR1693767) and North Sea (SRR20015061) to the mitochondrial genome of *O. dioica* revealed two regions with higher coverage that we inferred to be *rns* and *rnl* (supplementary Fig. S5, Supplementary Material online). Read mapping was done using the Geneious Mapper, Geneious Prime v.2023.2.1 with the parameters: medium-low sensitivity, randomly map multiple best matches, only map paired reads which both map, and trim paired reads overhangs. Average coverage was computed with Geneious Prime v.2023.2.1 statistics. The region that we annotated as *rnl* was also identified as such using gene prediction with MITOS v.2 (Donath, et al. 2019). The *rnl* and *rns* sequences were also present in the EST data, which helped determine the boundaries of these ribosomal genes.

tRNAs

Putative tRNAs were searched using MITOS v.2 (Donath, et al. 2019) and the ARWEN v.1.2 webserver (Laslett and Canbäck 2008). Both programs identify a single tRNA gene (supplementary Fig. S6, Supplementary Material online).

Aminoacyl-tRNA Synthetase Profiling

To corroborate the absence of tRNA genes in the mitochondrial genome, we searched for aaRS genes in the nuclear proteome (i.e., the amino acid sequences of *O. dioica* in the NCBI "protein" database). The aaRS search was done using HMMER v.3.3.2 software (Eddy 2011) and was based on profiles developed by Pett and Lavrov (2015). These profiles were used to search against proteome datasets downloaded from NCBI on April 2023 of *O. dioica* from Norway (GCA_000209535), *O. dioica* from Okinawa (GCA_907165135), *H. sapiens* (GCF_000001405.40 Human Build 38 patch release 14), *C. intestinalis* (GCF_000224145.3), and *S. clava* (GCF_013122585.1).

Nuclear Gene Transfer

We used HMM searches against the proteome of *O. dioica* from Norway GCA_000209535 and *O. dioica* from Okinawa GCA_907165135 to detect canonical mitochondrial-encoded genes that could have been transferred to the nuclear genomes. The searches were performed using HMMER v3.4 (Eddy 2011) using the *atp8*, *nad2*, *nad3*, *nad4L*, and *nad6* gene models developed by Gabriel Alves Vieira and available in the mitos2_wrapper source code repository (Vieira 2023). As negative control we also searched the proteomes of *H. sapiens* GCF_000001405.40 Human Build 38 patch release 14, *C. intestinalis* GCF_000224145.3, and *S. clava* GCF_013122585.1. Putative mitochondrial proteins that were found to be encoded in

the nuclear genome were searched for mitochondrial targeting signal using the TargetP-2.0 webserver (Armenteros, et al. 2019).

Codon Usage and Amino-Acid Composition

Codon usage and amino acid composition were computed using Geneious Prime v.2023.2.1.

Characterization of ODI_mt_ORF196

The number of transmembrane domains of ODI_mt_ORF196 was predicted using TMHMM v.1.0.2 in Geneious Prime v.2023.2.1 (Viklund and Elofsson 2004). The protein structure was predicted using Alphafold (Jumper, et al. 2021). The predicted structure was used as query against a large database of structures using Foldseek (van Kempen, et al. 2024).

Characterization of the Poly-T/A Stretches

We define poly-T stretches, by manually examining 59 cases of edited poly-T sites, i.e., these editing cases were validated by comparing RNA and DNA sequences of these loci. A classic poly-T stretch is defined as follows: (1) the 5'-end of this stretch starts with a perfect 6T homopolymer. This region is not excised; (2) downstream of this region, there is a C/T stretch (i.e., a Polypyrimidine track). This region is excised; (3) the stretch ends when either an A or a G nucleotide is encountered. This A or G nucleotide is not part of the poly-T stretch and not excised. In six validated cases, this pattern was violated. In five of these cases there was a single A nucleotide within the long C/T stretch, and in one case a G. We thus include in the definition cases in which the C/T stretch includes a single purine, as long as it is followed by at least 10 more C/T nucleotides. Searching the genome with this definition, we found six additional poly-T stretches (four classic and two non-classic) for which we lack RNA support. In total we annotated 65 poly-T stretches in these genomes. As we search for the above motif

or its reverse complement to account for both strands, we term these stretches poly-T/A stretches.

For each homopolymer site in the genome we extracted 50 bp before the site, the 6 T/A in the site itself, and 50 bp after the site using our own python v.3.11.5 script on Jupiter Notebook v.7.1.2. Nucleotide frequencies before and after the homopolymer sites were plotted (Supplementary Fig. S3, Supplementary Material online) by WebLogo with parameters of Advanced Logo Options: Frequency Plot.v.2.8.2 (Crooks, et al. 2004). To determine the conservation of the poly T/A stretches, we aligned the mitochondrial gene regions extracted from the Illumina RNA data from Japan and to our own assembly. Alignments were computed using MAFFT v.7.490 under the L-INS-i algorithm.

Mitochondrial Genome Length among Tunicates

The average mitochondrial genome size of tunicates was calculated from the length of the whole genome sequences of 34 tunicate species (supplementary table S3, Supplementary Material online) downloaded from the NCBI database.

Phylogenetic Analysis of Mitochondrial Protein Sequences

The phylogenetic analyses included 34 tunicate species with a complete mitochondrial genome that were deposited in NCBI (last accessed: June 2023) and 14 outgroup species (supplementary table S3, Supplementary Material online). The outgroup species were chosen following Bourlat, et al. (2006); Bourlat, et al. (2008); Shenkar, et al. (2016); Singh, et al. (2009). Eight protein-coding gene (*atp6, cox1, cox2, cox3, cytb, nad1, nad4, nad5*) were first extracted from each species and aligned separately. We used the Guidance2 server (Sela, et al. 2015) to identify unreliable regions of the alignment. We excluded these regions as well as

alignment columns that included more than 50% missing data or gaps. The different protein-coding alignments were then concatenated to form a super-matrix with 2,027 columns. Because members of the tunicate genus *Salpa* are extremely fast evolving, we prepared a second dataset, repeating the above steps, but excluding *S. thompsoni* and *S, fusiformi*. The resulting super-matrix of 46 species had 2,176 columns.

The phylogenetic trees were reconstructed under the maximum likelihood (ML) criterion using IQ-TREE 2.1.2 (Minh, et al. 2020). First, we identified the best-fitting model by using the ModelFinder-Plus (MFP) option of IQ-TREE 2.1.2 and computed the ML tree using this model. The model that best fitted both datasets (with and without the genus *Salpa*) was mtZOA+F+G+I. We reconstructed the tree using complex models that are not implemented in MFP: mtZOA+EHO+F+G+I, Poisson+C10+G, and Poisson+C20+G. The Robustness of each internal branch of the ML trees were evaluated with 100 bootstrap replications (Felsenstein 1985).

Bayesian tree reconstructions were performed using the site-heterogeneous CAT model implemented in Phylobayes MPI v1.5 (Lartillot, et al. 2013), which is expected to lower the impact of long-branch attraction on the phylogenetic tree inferred (Lartillot, et al. 2007). For the first and second datasets, four independent chains were run for 71,880 and 188,000 cycles, respectively. The first 5,000 and 10,000 trees from each chain, for the first and second data sets, respectively, were discarded as burn-in and trees were sampled every 10 trees (i.e., the sample size was 3,160, and 17,800 trees per chain for the first and second data set respectively). Chain convergence was assessed using the bpcomp and tracecomp scripts, which are part of Phylobayes. Specifically, the bpcomp maxdiff values were 0.23 and the tracecomp effsize and rel_diff values were >800 and below 0.15, supporting a proper convergence for the first dataset. For the second dataset, the bpcomp maxdiff value was 0.40 when the 4 chains were considered together, which indicated insufficient convergence.

However, when considering only chains 1, 2, and 3 or chains 1, 2 and 4 this value dropped to 0.18 and 0.27 indicating proper convergence. In both cases, rel_diff values were >150 and below 0.16 supporting convergence. We thus considered these two results.

Supplementary Material

Supplementary files Tables S1-S6. Figures S1-S10 are available at Genome Biology and Evolution online.

Acknowledgments

This work was supported by the German-Israeli Foundation for Scientific Research and Development to DH and TS (Grant No. I-1454-203.13/2018). We want to thank Nitzan Fourier from the Technion Genome Center for her help with Nanopore sequencing. We thank Yair Shimony for his help with the structure predictions.

Data Availability

The Illumina read data have been deposited in the European Nucleotide Archive under study ID number PRJEB72855. The mtDNA sequence was deposited under accession number OZ035851. The ONT reads obtained for each of the PCR fragments, as well as the sequences assembled from published RNA and EST data are available on GitHub (https://github.com/dorohuchon/Oikopleura_dioica_mitochondrial_genome).

Literature Cited

Adams KL, Palmer JD 2003. Evolution of mitochondrial gene content: gene loss and transfer to the nucleus. Mol Phylogenetics Evol. 29:380-395. https://doi.org/10.1016/S1055-7903(03)00194-5

Arafat H, Alamaru A, Gissi C, Huchon D 2018. Extensive mitochondrial gene rearrangements in Ctenophora: insights from benthic Platyctenida. BMC Evol Biol. 18:65. https://doi.org/10.1186/s12862-018-1186-1

Ari Ş, Arikan M. 2016. Next-generation sequencing: Advantages, disadvantages, and future. In: Hakeem KR, Tombuloğlu H, Tombuloğlu G, editors. Plant Omics: Trends and Applications. Springer International Publishing. 109-135. https://doi.org/10.1007/978-3-319-31703-8_5

Armenteros JJA, et al. 2019. Detecting sequence signals in targeting peptides using deep learning. Life Sci Alliance. 2:e201900429. https://doi.org/10.26508/lsa.201900429

Beagley CT, Okimoto R, Wolstenholme DR 1998. The mitochondrial genome of the sea anemone *Metridium senile* (Cnidaria): introns, a paucity of tRNA genes, and a near-standard genetic code. Genetics. 148:1091-1108. https://doi.org/10.1093/genetics/148.3.1091

Berná L, Alvarez-Valin F 2014. Evolutionary genomics of fast evolving tunicates. Genome Biol Evol 6:1724-1738. https://doi.org/10.1093/gbe/evu122

Bianchetti R, Lucchini G, Crosti P, Tortora P 1977. Dependence of mitochondrial protein synthesis initiation on formylation of the initiator methionyl-tRNAf. J Biol Chem. 252:2519-2523. https://doi.org/10.1016/S0021-9258(17)40489-3

Bliznina A, et al. 2021. Telomere-to-telomere assembly of the genome of an individual *Oikopleura dioica* from Okinawa using Nanopore-based sequencing. BMC Genom. 22:222. https://doi.org/10.1186/s12864-021-07512-6

Boore JL 1999. Animal mitochondrial genomes. Nucleic Acids Res. 27:1767-1780. https://doi.org/10.1093/nar/27.8.1767

Bouquet J-M, et al. 2009. Culture optimization for the emergent zooplanktonic model organism *Oikopleura dioica*. J Plankton Res. 31:359-370. https://doi.org/10.1093/plankt/fbn132

Bourlat SJ, et al. 2006. Deuterostome phylogeny reveals monophyletic chordates and the new phylum Xenoturbellida. Nature. 444:85-88. https://doi.org/10.1038/nature05241

Bourlat SJ, Nielsen C, Economou AD, Telford MJ 2008. Testing the new animal phylogeny: a phylum level molecular analysis of the animal kingdom. Mol Phylogenet Evol. 49:23-31. https://doi.org/10.1016/j.ympev.2008.07.008

Braun K, Leubner F, Stach T 2020. Phylogenetic analysis of phenotypic characters of Tunicata supports basal Appendicularia and monophyletic Ascidiacea. Cladistics. 36:259-300. https://doi.org/10.1111/cla.12405

Cardol P, et al. 2006. ND3 and ND4L subunits of mitochondrial complex I, both nucleus encoded in *Chlamydomonas reinhardtii*, are required for activity and assembly of the enzyme. Eukaryot Cell. 5:1460-1467. https://doi.org/10.1128/ec.00118-06

Castellana S, Vicario S, Saccone C 2011. Evolutionary patterns of the mitochondrial genome in Mtazoa: exploring the role of mutation and selection in mitochondrial protein–coding genes. Genome Biol Evol. 3:1067-1079. https://doi.org/10.1093/gbe/evr040

Chorev M, Carmel L 2012. The function of introns. Front Genet. 3:55. https://doi.org/10.3389/fgene.2012.00055

Connell GJ, Byrne EM, Simpson L 1997. Guide RNA-independent and guide RNA-dependent uridine insertion into *Cytochrome b* mRNA in a mitochondrial lysate from *Leishmania tarentolae*: role of RNA secondary structure. Biol Chem. 272:4212-4218. https://doi.org/10.1074/jbc.272.7.4212

Crooks GE, Hon G, Chandonia JM, Brenner SE 2004. WebLogo: a sequence logo generator. Genome Res. 14:1188-1190. https://doi.org/10.1101/gr.849004

Cruz-Reyes J, Sollner-Webb B 1996. Trypanosome U-deletional RNA editing involves guide RNA-directed endonuclease cleavage, terminal U exonuclease, and RNA ligase activities. Proc Natl Acad Sci USA. 93:8901-8906. https://doi.org/10.1073/pnas.93.17.8901

Danks G, et al. 2012. OikoBase: a genomics and developmental transcriptomics resource for the urochordate *Oikopleura dioica*. Nucleic Acids Res. 41:D845-D853. https://doi.org/10.1093/nar/gks1159

Delahaye C, Nicolas J 2021. Sequencing DNA with nanopores: troubles and biases. PLOS ONE. 16:e0257521. https://doi.org/10.1371/journal.pone.0257521

Delsuc F, Brinkmann H, Chourrout D, Philippe H 2006. Tunicates and not cephalochordates are the closest living relatives of vertebrates. Nature. 439:965-968. https://doi.org/10.1038/nature04336

Delsuc F, et al. 2018. A phylogenomic framework and timescale for comparative studies of tunicates. BMC Biol. 16. https://doi.org/10.1186/s12915-018-0499-2

Denoeud F, et al. 2010. Plasticity of animal genome architecture unmasked by rapid evolution of a pelagic tunicate. Science. 330:1381-1385. https://doi.org/10.1126/science.1194167

Donath A, et al. 2019. Improved annotation of protein-coding genes boundaries in metazoan mitochondrial genomes. Nucleic Acids Res. 47:10543-10552. https://doi.org/10.1093/nar/gkz833

Durrheim GA, Corfield VA, Harley EH, Ricketts MH 1993. Nucleotide sequence of cytochrome oxidase (subunit III) from the mitochondrion of the tunicate *Pyura*

stolonifera: evidence that AGR encodes glycine. Nucleic Acids Res. 21:3587-3588. https://doi.org/10.1093/nar/21.15.3587

Eddy SR 2011. Accelerated profile HMM searches. PLoS Comput Biol. 7:e1002195. . https://doi.org/10.1371/journal.pcbi.1002195

Erpenbeck D, et al. 2006. Mitochondrial diversity of early-branching metazoa is revealed by the complete mt genome of a haplosclerid demosponge. Mol Biol Evol 24:19-22. https://doi.org/10.1093/molbev/msl154

Felsenstein J 1985. Confidence limits on phylogenies: an approach using the bootstrap. Evolution. 39:783-791. https://doi.org/10.2307/2408678

Fulton TL, Wagner SM, Shapiro B. 2012. Case study: recovery of ancient nuclear DNA from toe pads of the extinct passenger pigeon. In: Shapiro B, Hofreiter M, editors. Ancient DNA: methods and protocols. Humana Press. 29-35. https://doi.org/10.1007/978-1-61779-516-9_4

Garić R 2024. World List of Appendicularia. Appendicularia. Accessed through: World Register of Marine Species. https://www.marinespecies.org/aphia.php?p=taxdetails&id=146421

Garić R, et al. 2018. Challenges in appendicularian integrative taxonomy and barcoding // ICES Annual Science Conference 2018. https://www.imp-du.com/datoteke/Ices-2018-rade-garic.pdf

Gissi C, Iannelli F, Pesole G 2004. Complete mtDNA of *Ciona intestinalis* reveals extensive gene rearrangement and the presence of an *atp8* and an extra *trnM* gene in ascidians. J Mol Evol. 58:376-389. https://doi.org/10.1007/s00239-003-2559-6

Gissi C, Iannelli F, Pesole G 2008. Evolution of the mitochondrial genome of Metazoa as exemplified by comparison of congeneric species. Heredity. 101:301-320. https://doi.org/10.1038/hdy.2008.62

Gissi C, Pesole G 2003. Transcript mapping and genome annotation of ascidian mtDNA using EST data. Genome Res. 13:2203-2212. https://doi.org/10.1101/gr.1227803

Gott JM, Emeson RB 2000. Functions and mechanisms of RNA editing. Annu Rev Genet. 34:499-531. https://doi.org/10.1146/annurev.genet.34.1.499

Helfenbein KG, Fourcade HM, Vanjani RG, Boore JL 2004. The mitochondrial genome of *Paraspadella goto* is highly reduced and reveals that chaetognaths are a sister group to protostomes. Proc Natl Acad Sci USA. 101:10639-10643. https://doi.org/10.1073/pnas.0400941101

Hoffmann RJ, Boore JL, Brown WM 1992. A novel mitochondrial genome organization for the blue mussel, *Mytilus edulis*. Genetics. 131:397-412. https://doi.org/10.1093/genetics/131.2.397

Iannelli F, Griggio F, Pesole G, Gissi C 2007. The mitochondrial genome of *Phallusia mammillata* and *Phallusia fumigata* (Tunicata, Ascidiacea): high genome plasticity at intra-genus level. BMC Evol Biol. 7:155. https://doi.org/10.1186/1471-2148-7-155

Jumper J, et al. 2021. Highly accurate protein structure prediction with AlphaFold. Nature. 596:583-589. https://doi.org/10.1038/s41586-021-03819-2

Kolmogorov M, et al. 2020. metaFlye: scalable long-read metagenome assembly using repeat graphs. Nat Methods. 17:1103-1110. https://doi.org/10.1038/s41592-020-00971-x

Lartillot N, Brinkmann H, Philippe H 2007. Suppression of long-branch attraction artefacts in the animal phylogeny using a site-heterogeneous model. BMC Evol Biol. 7:S4. https://doi.org/10.1186/1471-2148-7-S1-S4

Lartillot N, Philippe H 2004. A bayesian mixture model for across-site heterogeneities in the amino-acid replacement process. Mol Biol Evol. 21:1095-1109. https://doi.org/10.1093/molbev/msh112

Lartillot N, Rodrigue N, Stubbs D, Richer J 2013. PhyloBayes MPI: Phylogenetic reconstruction with infinite mixtures of profiles in a parallel environment. Syst Biol. 62:611-615. https://doi.org/10.1093/sysbio/syt022

Laslett D, Canbäck B 2008. ARWEN: a program to detect tRNA genes in metazoan mitochondrial nucleotide sequences. Bioinformatics. 24:172-175. https://doi.org/10.1093/bioinformatics/btm573

Latour AR 2021. Molecular divergence and gene flow in cold ocean tunicates: insights from cytochrome oxidase 1. Diss Memorial University of Newfoundland.73-87. https://doi.org/10.48336/hkd1-9x29

Lavrov DV 2007. Key transitions in animal evolution: a mitochondrial DNA perspective. Integr Comp Biol. 47:734-743. https://doi.org/10.1093/icb/icm045

Lavrov DV, Adamski M, Chevaldonné P, Adamska M 2016. Extensive mitochondrial mRNA editing and unusual mitochondrial genome organization in calcaronean sponges. Curr Biol. 26:86-92. https://doi.org/10.1016/j.cub.2015.11.043

Lavrov DV, et al. 2023. Phylomitogenomics bolsters the high-level classification of Demospongiae (phylum Porifera). PLOS ONE. 18:e0287281. https://doi.org/10.1371/journal.pone.0287281

Lavrov DV, Pett W 2016. Animal mitochondrial DNA as we do not know it: mt-genome organization and evolution in nonbilaterian lineages. Genome Biol Evol. 8:2896-2913. https://doi.org/10.1093/gbe/evw195

Le TH, Blair D, McManus DP 2002. Mitochondrial genomes of parasitic flatworms. Trends Parasitol. 18:206-213. https://doi.org/10.1016/S1471-4922(02)02252-3

Lonergan KM, Gray MW 1996. Expression of a continuous open reading frame encoding subunits 1 and 2 of cytochrome *c* oxidase in the mitochondrial DNA of *Acanthamoeba castellanii*. J Mol Biol. 257:1019-1030. https://doi.org/10.1006/jmbi.1996.0220

Martin M 2011. Cutadapt removes adapter sequences from high-throughput sequencing reads. EMBnet j. 17:3. https://doi.org/10.14806/ej.17.1.200

Masunaga A, et al. 2022. The cosmopolitan appendicularian *Oikopleura dioica* reveals hidden genetic diversity around the globe. Mar Biol. 169:157. https://doi.org/10.1007/s00227-022-04145-5

Minh BQ, et al. 2020. IQ-TREE 2: New models and efficient methods for phylogenetic inference in the genomic era. Mol Biol Evol. 37:1530-1534. https://doi.org/10.1093/molbev/msaa015

Naville M, et al. 2019. Massive changes of genome size driven by expansions of non-autonomous transposable elements. Curr Biol. 29:1161-1168.e1166. https://doi.org/10.1016/j.cub.2019.01.080

Nishida H 2008. Development of the appendicularian *Oikopleura dioica*: culture, genome, and cell lineages. Dev Growth Differ. 50:S239-S256. https://doi.org/10.1111/j.1440-169X.2008.01035.x

Ojala D, Montoya J, Attardi G 1981. tRNA punctuation model of RNA processing in human mitochondria. Nature. 290:470-474. https://doi.org/10.1038/290470a0

Okimoto R, Macfarlane JL, Clary DO, Wolstenholme DR 1992. The mitochondrial genomes of two nematodes, *Caenorhabditis elegans* and *Ascaris suum*. Genetics. 130:471-498. https://doi.org/10.1093/genetics/130.3.471

Pesole G, Gissi C, De Chirico A, Saccone C 1999. Nucleotide substitution rate of mammalian mitochondrial genomes. J Mol Evol. 48:427-434. https://doi.org/10.1007/PL00006487

Pett W, Lavrov DV 2015. Cytonuclear interactions in the evolution of animal mitochondrial tRNA metabolism. Genome Biol Evol. 7:2089-2101. https://doi.org/10.1093/gbe/evv124

Pett W, et al. 2011. Extreme mitochondrial evolution in the ctenophore *Mnemiopsis leidyi*: Insight from mtDNA and the nuclear genome. Mitochondrial DNA. 22:130-142. https://doi.org/10.3109/19401736.2011.624611

Philippe H, Zhou Y, Brinkmann H, Rodrigue N, Delsuc F 2005. Heterotachy and long-branch attraction in phylogenetics. BMC Evol Biol. 5:50. https://doi.org/10.1186/1471-2148-5-50

Pichon J, Luscombe NM, Plessy C 2020. Widespread use of the "ascidian" mitochondrial genetic code in tunicates. F1000Research. 8:2072-2072. 10.12688/f1000research.21551.2

Pichon J, Luscombe NM, Plessy C 2019. Widespread use of the "ascidian" mitochondrial genetic code in tunicates. F1000Research. 8:2072-2072. https://doi.org/10.12688%2Ff1000research.21551.2

Raghavan V, Eichele G, Larink O, Karin EL, Söding J 2023. RNA sequencing indicates widespread conservation of circadian clocks in marine zooplankton. NAR Genom Bioinform. 5. https://doi.org/10.1093/nargab/lqad007

Rogozin IB, Carmel L, Csuros M, Koonin EV 2012. Origin and evolution of spliceosomal introns. Biol Direct. 7:11. https://doi.org/10.1186/1745-6150-7-11

Rubinstein ND, et al. 2013. Deep sequencing of mixed total DNA without barcodes allows efficient assembly of highly plastic ascidian mitochondrial genomes. Genome Biol Evol. 5:1185-1199. https://doi.org/10.1093/gbe/evt081

Sela I, Ashkenazy H, Katoh K, Pupko T 2015. GUIDANCE2: Accurate detection of unreliable alignment regions accounting for the uncertainty of multiple parameters. Nucleic Acids Res. 43:W7-W14. https://doi.org/10.1093/nar/gkv318

Sereika M, et al. 2022. Oxford Nanopore R10.4 long-read sequencing enables the generation of near-finished bacterial genomes from pure cultures and metagenomes without

short-read or reference polishing. Nat Methods. 19:823-826. https://doi.org/10.1038/s41592-022-01539-7

Shenkar N, Koplovitz G, Dray L, Gissi C, Huchon D 2016. Back to solitude: Solving the phylogenetic position of the diazonidae using molecular and developmental characters. Mol Phylogenetics Evol. 100:51-56. https://doi.org/10.1016/j.ympev.2016.04.001

Singh TR, et al. 2009. Tunicate mitogenomics and phylogenetics: peculiarities of the *Herdmania momus* mitochondrial genome and support for the new chordate phylogeny. BMC Genom. 10:534. https://doi.org/10.1186/1471-2164-10-534

Spealman P, Burrell J, Gresham D 2020. Inverted duplicate DNA sequences increase translocation rates through sequencing nanopores resulting in reduced base calling accuracy. Nucleic Acids Res. 48:4940-4945. https://doi.org/10.1093/nar/gkaa206

Stach T, Braband A, Podsiadlowski L 2010. Erosion of phylogenetic signal in tunicate mitochondrial genomes on different levels of analysis. Mol Phylogenetics Evol. 55:860-870. https://doi.org/10.1016/j.ympev.2010.03.011

The UniProt Consortium 2022. UniProt: the universal protein knowledgebase in 2023. Nucleic Acids Res. 51:D523-D531. https://doi.org/10.1093/nar/gkac1052

van Kempen M, et al. 2024. Fast and accurate protein structure search with Foldseek. Nature Biotechnology. 42:243-246. https://doi.org/10.1038/s41587-023-01773-0

[source code repository] Vieira GA. 2023. mitos2_wrapper. GitHub. https://github.com/gavieira/mitos2_wrapper/tree/master/refseq63m/featureProtHMM.

Viklund H, Elofsson A 2004. Best alpha-helical transmembrane protein topology predictions are achieved using hidden Markov models and evolutionary information. Prot Sci. 13:1908-1917. https://doi.org/10.1110/ps.04625404

Wang H-C, Minh BQ, Susko E, Roger AJ 2017. Modeling site heterogeneity with posterior mean site frequency profiles accelerates accurate phylogenomic estimation. Syst Biol. 67:216-235. https://doi.org/10.1093/sysbio/syx068

Wang J, et al. 2022. The conserved domain database in 2023. Nucleic Acids Res. 51:D384-D388. https://doi.org/10.1093/nar/gkac1096

Wang K, Omotezako T, Kishi K, Nishida H, Onuma TA 2015. Maternal and zygotic transcriptomes in the appendicularian, *Oikopleura dioica*: novel protein-encoding genes, intra-species sequence variations, and trans-spliced RNA leader. Dev Genes Evol. 225:149-159. https://doi.org/10.1007/s00427-015-0502-7

Waring RB, Davies RW 1984. Assessment of a model for intron RNA secondary structure relevant to RNA self-splicing - a review. Gene. 28:277-291. https://doi.org/10.1016/0378-1119(84)90145-8

Wick RR, Judd LM, Gorrie CL, Holt KE 2017. Completing bacterial genome assemblies with multiplex MinION sequencing. Microb Genom. 3:e000132. https://doi.org/10.1099/mgen.0.000132

Wick RR, Judd LM, Holt KE 2019. Performance of neural network basecalling tools for Oxford Nanopore sequencing. Genome Biol. 20:129. https://doi.org/10.1186/s13059-019-1727-y

Yahalomi D, et al. 2017. The multipartite mitochondrial genome of *Enteromyxum leei* (Myxozoa): eight fast-evolving megacircles. Mol Biol Evol. 34:1551–1556. https://doi.org/10.1093/molbev/msx072

Yokobori S-i, et al. 1999. Complete DNA sequence of the mitochondrial genome of the ascidian *Halocynthia roretzi* (Chordata, Urochordata). Genetics. 153:1851-1862. https://doi.org/10.1093/genetics/153.4.1851

Yokobori S-i, Ueda T, Watanabe K 1993. Codons AGA and AGG are read as glycine in ascidian mitochondria. J Mol Evol. 36:1-8. https://doi.org/10.1007/BF02407301

Yokobori S-i, Watanabe Y, Oshima T 2003. Mitochondrial genome of *Ciona savignyi* (Urochordata, Ascidiacea, Enterogona): comparison of gene arrangement and tRNA genes with *Halocynthia roretzi* mitochondrial genome. J Mol Evol. 57:574-587. https://doi.org/10.1007/s00239-003-2511-9

Zhu W, Lomsadze A, Borodovsky M 2010. *Ab initio* gene identification in metagenomic sequences. Nucleic Acids Res. 38:e132-e132. https://doi.org/10.1093/nar/gkq275

Figure legend

Figure 1. *Oikopleura dioica* mitochondrial genome map.

Protein-coding genes are in green, rRNA genes (*rns*, *rnl*) are in dark blue, tRNA-Met (UAU) is in pink, coding sequences (CDS) are in yellow, and the poly-T/A stretches are in light blue. The genes are pointing in the direction of their transcriptional orientation. A non-sequenced region is indicated as "gap" is in gray.

Figure 2. A typical poly-T/A region in *O. doica cox1* gene.

The reference sequence represents the assembled mitochondrial genome. The sequence of part of the *cox1* gene is indicated in dark green. Above it are the nucleotide and amino-acid sequences of the reference sequence. In light blue is the poly-T/A region. Reads from five different sequencing sources mapped to this region are shown below the reference sequence: our ONT data, our Illumina reads, public EST data from Norway, public RNA reads from Japan, and public RNA reads from the North Sea (see Supplementary table S3, Supplementary Material online A for accession numbers). Each line represents a different read. Note that the different ONT reads do not have the same length, exemplifying the fact that the length of the poly-T region could not be accurately determined. The EST and RNA reads lack a long poly-T region. Rather, the poly-T region corresponds to 6U-bases. This difference (long poly-T stretch in DNA *versus* 6U in the EST and RNA reads) provides evidence for editing at the RNA level. Illumina reads can map to each side of the poly-T stretch, but because poly-T stretches can be longer than the read length, we are unable to assemble the entire region using Illumina only or determine the length of the poly-T region.

Figure 3. Presence-absence of aaRS orthologs in different species.

Single eukaryotic (Euk): single copy aaRSs that function both in the cytosol and mitochondria. Other aaRSs are either expressed only in the cytosol (cytosolic) or in the mitochondrion (mitochondrial). In pink aaRSs presence, in white absence, and in blue the aaRS-Gly. Protein accession numbers are provided in Supplementary table S3, Supplementary Material online.

Figure 4. The position of *O. dioica* among chordates.

The phylogenetic tree was reconstructed based on mitochondrial protein sequences. Branch supports are only indicated for those cases in which the bootstrap support values were lower than 100%. The tunicates classes: Stolidobranchia in blue, Thaliacea in red, Phlebobranchia in green, Aplousobranchia in yellow, and Appendicularia in purple.

Table

Table 1. *Oikopleura dioica* genes, position, length, direction (F- forward, R- reverse), start and stop codons, and comparison to the minimal, maximal, and average length of orthologous genes in 38 tunicate sequences (supplementary table S4, Supplementary Material online).

		Position		Length [bp]		Direction	Codon		Length range in tunicates [bp]		Average length in tunicates [bp]
Gene	**Type**	**start**	**end**	**gene**	**CDS**		**start**	**stop**	**min**	**max**	
srnl	rRNA	13	303	291	242	R			921	1,299	1,105
nad4	gene	934	2,847	1,914	876	R	ATC	TAA	1,209	1,401	1,321
cox3	gene	2,906	4,574	1,669	870	F	ATT	TAA	768	795	786
tRNA-M	tRNA	4,671	4,763	93	69	F			61	76	66
nad1	gene	4,805	5,800	996	615	F	TTG	TAA	853	1,035	914
cox1	gene	5,836	7,834	1,999	1,512	F	ATT	TAG	1,482	1,575	1,546
ODI_mt_ ORF196	gene	8,462	9,887	1,426	591	R	TTG	TAA			
cytb	gene	10,115	12,085	1,971	993	F	GTG	TAA	1,035	1,122	1,093
atp6	gene	12,312	13,063	752	516	R	ATT	TAA	492	642	619
rns	rRNA	13,064	13,295	232	215	R			596	984	696
cox2	gene	13,305	14,301	997	582	F	ATT	TAA	651	942	689
nad5	gene	14,456	18,371	3,916	1,248	F	ATA	TAA	1,458	1,788	1,695

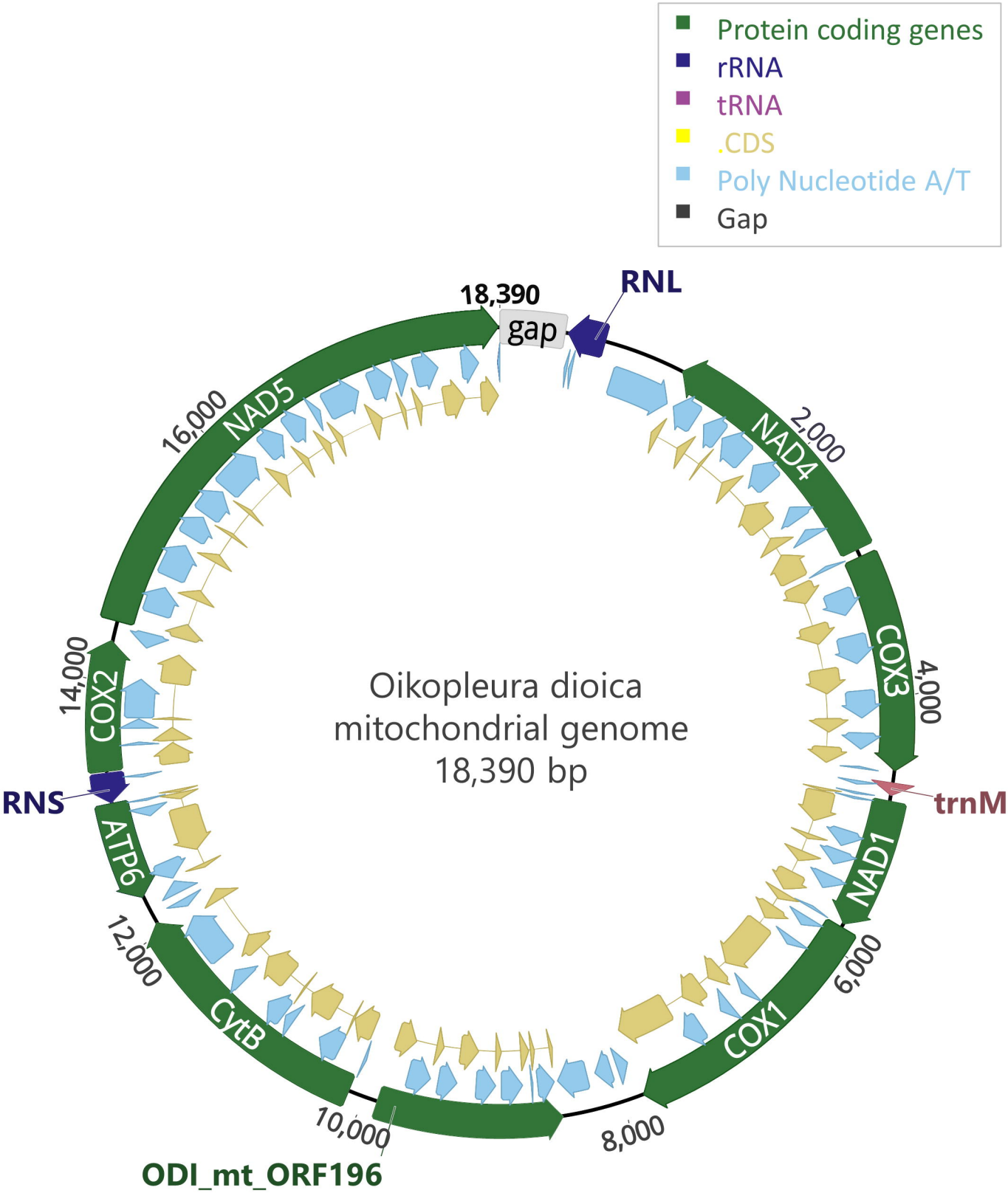
Protein coding genes
rRNA
tRNA
.CDS
Poly Nucleotide A/T
Gap
Oikopleura dioica
mitochondrial genome
18,390 bp
18,390
gap
RNL
NAD4
2,000
COX3
4,000
trnM
NAD1
6,000
COX1
8,000
10,000
ODI_mt_ORF196
CytB
12,000
ATP6
RNS
COX2
14,000
NAD5
16,000

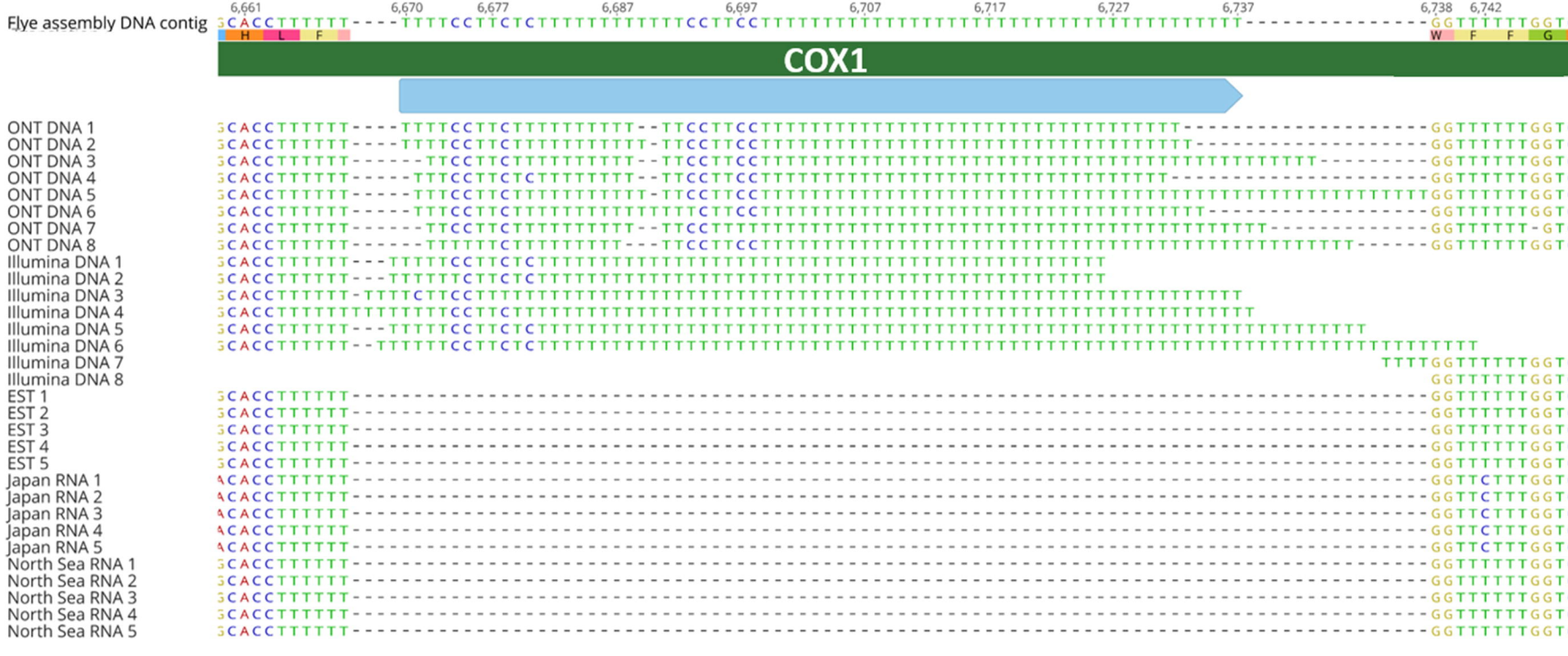
6,661
6,670
6,677
6,687
6,697
6,707
6,717
6,727
6,737
6,738
6,742
Flye assembly DNA contig
H
L
F
W
F
F
G
COX1
ONT DNA 1
ONT DNA 2
ONT DNA 3
ONT DNA 4
ONT DNA 5
ONT DNA 6
ONT DNA 7
ONT DNA 8
Illumina DNA 1
Illumina DNA 2
Illumina DNA 3
Illumina DNA 4
Illumina DNA 5
Illumina DNA 6
Illumina DNA 7
Illumina DNA 8
EST 1
EST 2
EST 3
EST 4
EST 5
Japan RNA 1
Japan RNA 2
Japan RNA 3
Japan RNA 4
Japan RNA 5
North Sea RNA 1
North Sea RNA 2
North Sea RNA 3
North Sea RNA 4
North Sea RNA 5

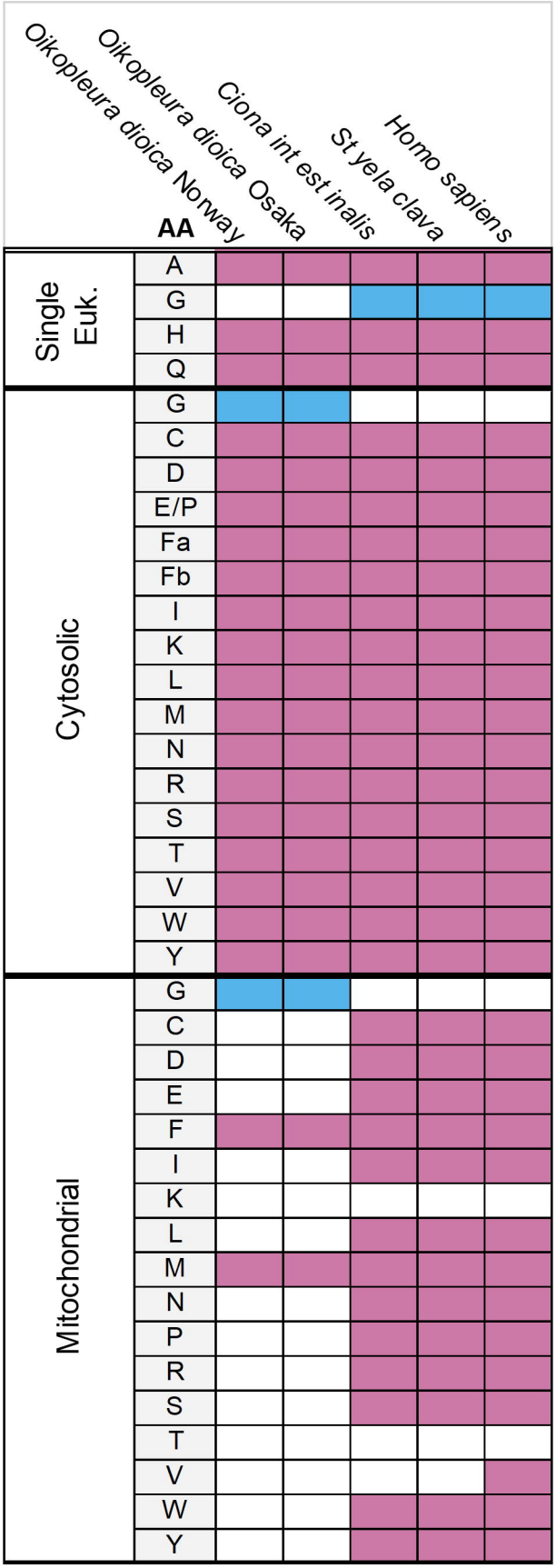
Oikopleura dioica Norway
Oikopleura dioica Osaka
Ciona intestinalis
Styela clava
Homo sapiens
AA
Single Euk.
A
G
H
Q
Cytosolic
G
C
D
E/P
Fa
Fb
I
K
L
M
N
R
S
T
V
W
Y
Mitochondrial
G
C
D
E
F
I
K
L
M
N
P
R
S
T
V
W
Y

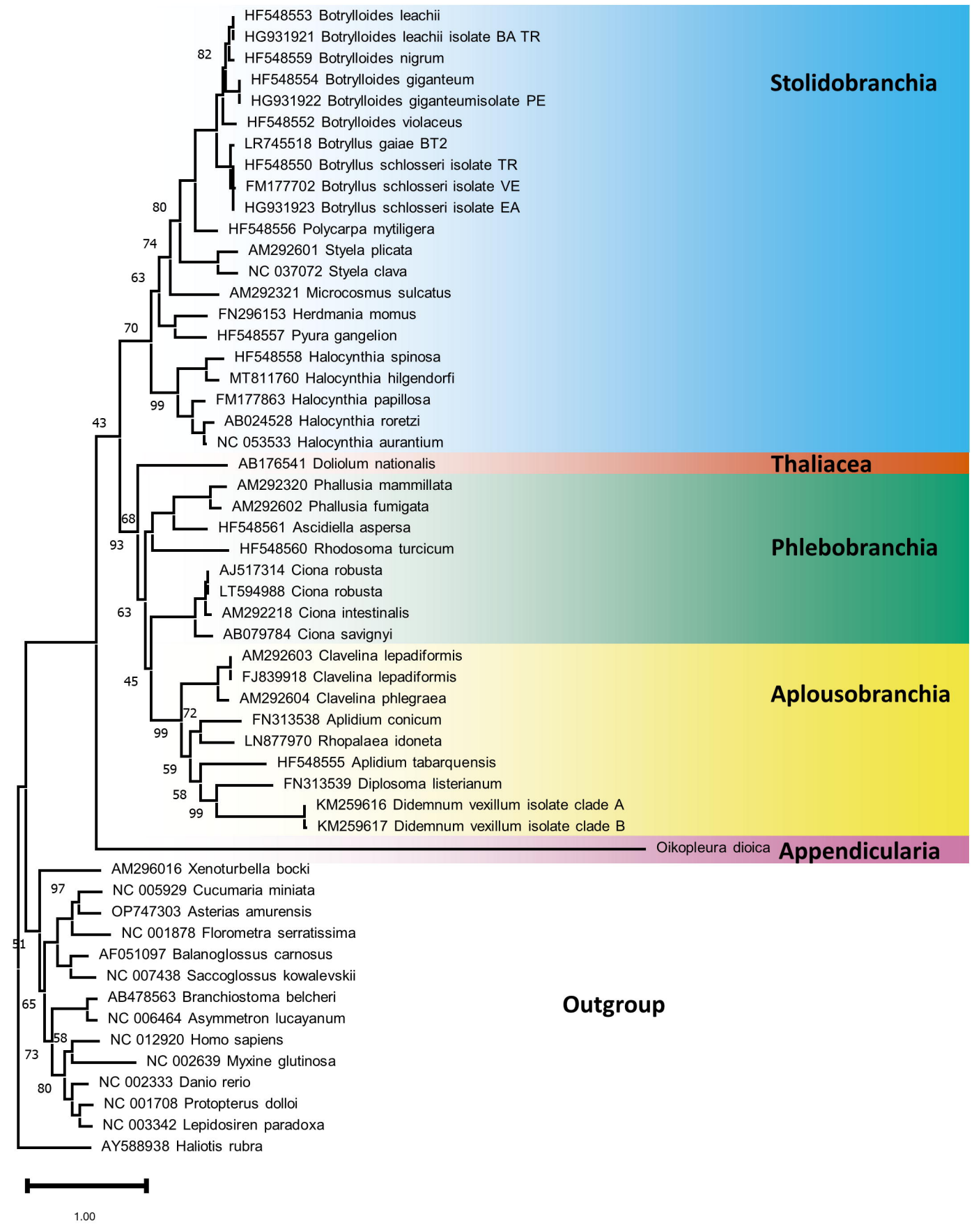
HF548553 Botrylloides leachii
HG931921 Botrylloides leachii isolate BA TR
HF548559 Botrylloides nigrum
HF548554 Botrylloides giganteum
HG931922 Botrylloides giganteumisolate PE
HF548552 Botrylloides violaceus
LR745518 Botryllus gaiae BT2
HF548550 Botryllus schlosseri isolate TR
FM177702 Botryllus schlosseri isolate VE
HG931923 Botryllus schlosseri isolate EA
HF548556 Polycarpa mytiligera
AM292601 Styela plicata
NC 037072 Styela clava
AM292321 Microcosmus sulcatus
FN296153 Herdmania momus
HF548557 Pyura gangelion
HF548558 Halocynthia spinosa
MT811760 Halocynthia hilgendorfi
FM177863 Halocynthia papillosa
AB024528 Halocynthia roretzi
NC 053533 Halocynthia aurantium
AB176541 Doliolum nationalis
AM292320 Phallusia mammillata
AM292602 Phallusia fumigata
HF548561 Ascidiella aspersa
HF548560 Rhodosoma turcicum
AJ517314 Ciona robusta
LT594988 Ciona robusta
AM292218 Ciona intestinalis
AB079784 Ciona savignyi
AM292603 Clavelina lepadiformis
FJ839918 Clavelina lepadiformis
AM292604 Clavelina phlegraea
FN313538 Aplidium conicum
LN877970 Rhopalaea idoneta
HF548555 Aplidium tabarquensis
FN313539 Diplosoma listerianum
KM259616 Didemnum vexillum isolate clade A
KM259617 Didemnum vexillum isolate clade B
Oikopleura dioica
AM296016 Xenoturbella bocki
NC 005929 Cucumaria miniata
OP747303 Asterias amurensis
NC 001878 Florometra serratissima
AF051097 Balanoglossus carnosus
NC 007438 Saccoglossus kowalevskii
AB478563 Branchiostoma belcheri
NC 006464 Asymmetron lucayanum
NC 012920 Homo sapiens
NC 002639 Myxine glutinosa
NC 002333 Danio rerio
NC 001708 Protopterus dolloi
NC 003342 Lepidosiren paradoxa
AY588938 Haliotis rubra
82
80
74
63
70
99
43
68
93
63
45
72
99
59
58
99
97
51
65
58
73
80
Stolidobranchia
Thaliacea
Phlebobranchia
Aplousobranchia
Appendicularia
Outgroup
1.00